

Magnetic properties of La_2CuMnO_6 double perovskite ceramic investigated by Monte Carlo simulations

S Mtougui, I EL Housni, N EL Mekkaoui, S Ziti, S Idrissi, H Labrim, R Khalladi, L Bahmad
Citation: Chin. Phys. B . 2020, 29(5): 056101 . **doi:** 10.1088/1674-1056/ab7d95
Journal homepage: http://cpb.iphy.ac.cn; http://iopscience.iop.org/cpb

What follows is a list of articles you may be interested in

Theoretical study on order-disorder phase transition of $CH_3NH_3PbCl_3$

Jing Chang(常静), Zhen-Yi Jiang(姜振益), Qi Song(宋齐), Lei Chen(陈磊), Yan-Min Lin(林彦明), Bo Zhou(周波)
Chin. Phys. B . 2019, 28(11): 116105 . **doi:** 10.1088/1674-1056/ab478d

Effect of particle size distribution on magnetic behavior of nanoparticles with uniaxial anisotropy

S Rizwan Ali, Farah Naz, Humaira Akber, M Naeem, S Imran Ali, S Abdul Basit, M Sarim, Sadaf Qaseem
Chin. Phys. B . 2018, 27(9): 097503 . **doi:** 10.1088/1674-1056/27/9/097503

Jamming of packings of frictionless particles with and without shear

Wen Zheng(郑文), Shiyun Zhang(张世允), Ning Xu(徐宁)
Chin. Phys. B . 2018, 27(6): 066102 . **doi:** 10.1088/1674-1056/27/6/066102

Effect of exchange interaction in ferromagnetic superlattices: A Monte Carlo study

R Masrour, A Jabar
Chin. Phys. B . 2016, 25(10): 107502 . **doi:** 10.1088/1674-1056/25/10/107502

Monte Carlo study of nanowire magnetic properties

R. Masrour, L. Bahmad, A. Benyoussef
Chin. Phys. B . 2013, 22(5): 057504 . **doi:** 10.1088/1674-1056/22/5/057504

Magnetic properties of La_2CuMnO_6 double perovskite ceramic investigated by Monte Carlo simulations

S Mtougui[1,†], I EL Housni[1], N EL Mekkaoui[1], S Ziti[2], S Idrissi[1], H Labrim[3], R Khalladi[1], and L Bahmad[1,‡]

[1] *Laboratoire de la Matière Condensée et des Sciences Interdisciplinaires (LaMCScI), Mohammed V University of Rabat, Faculty of Sciences, B.P.* 1014 *Rabat, Morocco*

[2] *Intelligent Processing and Security Systems, Mohammed V University of Rabat, Faculty of Sciences, B.P.* 1014 *Rabat, Morocco*

[3] *USM/DERS/Centre National de l'Energie, des Sciences et des Techniques Nucléaires (CNESTEN), Rabat, Morocco*

(Received 12 November 2019; revised manuscript received 14 February 2020; accepted manuscript online 9 March 2020)

We present a theoretical study of the magnetic properties of the lanthanum copper manganate double perovskite La_2CuMnO_6 ceramic, using Monte Carlo simulations. We analyze and discuss the ground state phase diagrams in different planes to show the effect of every physical parameter. Based on the Monte Carlo simulations, which combine Metropolis algorithm and Ising model, we explore the thermal behavior of the total magnetization and susceptibility. We also present and discuss the influence of physical parameters such as the external magnetic field, the exchange coupling interactions between magnetic atoms, and the exchange magnetic field on the magnetization of the system. Moreover, the critical temperature of the system is about $T_c = 70$ K, in agreement with the experimental value. Finally, the hysteresis loops of La_2CuMnO_6 are discussed.

Keywords: double perovskite La_2CuMnO_6, Monte Carlo simulations, Ising model, hysteresis loops, Metropolis algorithm, critical temperature

PACS: 61.43.Bn, 75.75.–c, 67.30.er, 76.60.Jx **DOI:** 10.1088/1674-1056/ab7d95

1. Introduction

Double perovskites with chemical formula $A_2B'B''O_6$, have attracted considerable interest because of their electrical and unique interesting magnetic properties. These materials have significant potential for technological applications.[1,2] The stability of the double perovskite materials depends on the choice of the $B'B''$ compounds, the degree of cation inversion, and the size of the transition metal cations B' and B''.[3] The double perovskites consist of two alternating simple octahedra perovskites, $B'O_6$ and $B''O_6$, which form two interspersed sublattices.[4–6]

Recently, researchers studied many double perovskites to investigate materials combining magnetic and electric properties, which can be used for non-volatile memories. The presence of both magnetic and dielectric properties makes the double perovskite oxides interesting, and encourages developing new materials with large scientific and novel technological impact.[7,8]

In our recent works, we touched on the magnetic properties of the perovskite family. The magnetic properties of the simple perovskites $BiFeO_3$,[9] $CeFeO_3$,[10] and $CeCrO_3$[11] and the triple perovskite $LaSr_2Cr_3O_9$[12] were deeply investigated, hence giving the motivation to explore other compounds.

In the same way, we explore the double perovskite La_2CuMnO_6 because of the multi-valences of the Mn ions: Mn^{2+}, Mn^{3+}, and Mn^{4+}. This compound is considered as one of the most useful additives. The MnO_2 can be used as a hard or soft additive doping element.[13] The double perovskites composed by rare earth and manganite have multiple functions and various device applications.[2] Recent studies reported that La_2NiMnO_6 is a ferromagnetic semiconductor, and is one of the most promising materials for spintronic devices.[2] Other studies on the properties of the double perovskite La_2CoMnO_6 showed that the compound presents a good ferromagnetic and insulating behavior.[1] Later, researchers found that replacing Co in La_2CoMnO_6 by Cu is more advantageous for spintronic devices. Recently, a synthesis of the lanthanum copper manganate double perovskite La_2CuMnO_6 demonstrated different typical behaviors, such as ferromagnetism and magnetoresistance.[14,15] To identify the crystalline structure and give information about the unit cell dimensions of the double perovskite La_2CuMnO_6, an x-ray diffraction has been used. This diffraction showed that the La_2CuMnO_6 crystallizes belong to an orthorhombic *Pbnm* space group, with Laue symmetry *mmm*. Some recent studies suggested the existing of a superexchange coupling between the Cu^{+2} and Mn^{+4} ions, Cu^{+2}–O–Mn^{+4}.[16] The presence of Cu^{2+} ion expects a strong Jahn–Teller effect and distortion due to the unevenly occupied e_g orbitals.[17] The ions Mn^{4+} ($S = 3/2$, $t_{2g}^3 e_g^0$) and Cu^{2+} ($t_{2g}^6 e_g^3$) have a superexchange ferromagnetic interaction.[17]

Motivated by the lack of the theoretical investigations

†Corresponding author. E-mail: sara.mtougui@gmail.com

‡Corresponding author. E-mail: lahou2002@gmail.com

© 2020 Chinese Physical Society and IOP Publishing Ltd

of the double perovskite ceramics La_2CuMnO_6, we study a model describing the critical behavior of the studied compound. In this work, based on Monte Carlo simulations, which have been performed under Metropolis algorithm,[18–22] we provide the magnetic properties in a wide temperature and external magnetic field range.

2. Model and simulation method

To inspect the magnetic behavior of the double perovskite La_2CuMnO_6, we carry out the Monte Carlo simulations under Metropolis algorithm. The studied compound consists of the Cu/MnO_6 octahedrons. The Cu/MnO_6 sublattices are shown in Fig. 1(b), using VESTA software.[23]

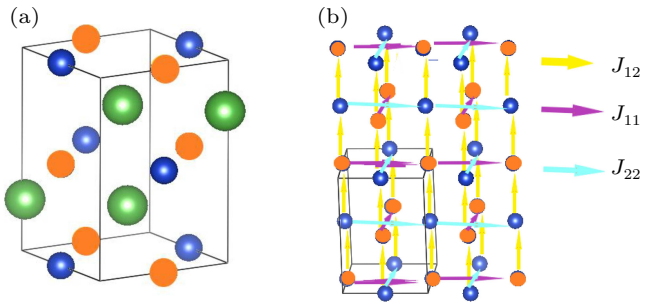


Fig. 1. (a) The crystal structure of La_2CuMnO_6, green atoms represent La cations, blue spheres represent Cu cations, and orange spheres are Mn atoms. (b) The magnetic structure showing only the Cu/Mn magnetic atoms and exchange coupling constants between atoms.

Table 1. The atom positions in the double perovskite La_2CuMnO_6.[15]

Atom	Site	x	y	z	B_{iso}/Å
La	4c	−0.00220	0.52107	0.25000	0.00213
Cu	4b	0.00000	0.00000	0.50000	0.00487
Mn	4b	0.00000	0.00000	0.50000	0.00487
O1	4c	0.48095	0.2500	−0.06812	0.01850
O2	8c	0.27475	0.03875	0.71424	0.00454

The Hamiltonian describing this system is based on different intrinsic parameters such as the spins, the exchange coupling constants, the crystal field and the extrinsic ones like the external magnetic field.[24–26] The critical behaviors of the double perovskite ceramic La_2CuMnO_6 are controlled by the following Hamiltonian:

$$H_S = -J_{11}\sum_{\langle i,j\rangle} S_iS_j - J_{22}\sum_{\langle k,l\rangle}\sigma_k\sigma_l - J_{12}\sum_{\langle m,n\rangle} S_m\sigma_n - D_S\sum_i S_i^2 - D_\sigma\sum_i\sigma_i^2 - H\left(\sum_i (S_i+\sigma_i)\right), \quad (1)$$

where $\langle i,j\rangle$ stands for the first nearest neighbors of the spins (Mn–Mn), $\langle k,l\rangle$ stands the first nearest neighbors of the spins (Cu–Cu), $\langle m,n\rangle$ stands the first nearest neighbors of the spins (Mn–Cu), J_{11} is the exchange coupling interaction between Mn–Mn atoms, J_{22} represents the exchange coupling interaction between Cu–Cu atoms, J_{12} stands for the exchange coupling interaction between Mn–Cu atoms, D represents the crystal field acting on the sublattices Cu/MnO_6, and H is the external magnetic field.

The calculation will be fixed for a specific system size, $N = 5\times5\times5$, using the free boundary conditions. We calculate first the total magnetizations, which correspond to the magnetization per site

$$M_T = \frac{1}{N}\left\langle\sum_i S_i\right\rangle. \quad (2)$$

After that, we calculate the magnetic susceptibility

$$\chi = \frac{1}{k_BT}\left(\langle M_T^2\rangle - \langle M_T\rangle^2\right), \quad (3)$$

where k_B is the Boltzmann constant. For simplicity, we take $k_B = 1$ in all the following calculations.

3. Results and discussion

To analyze and discuss the ground state phase diagrams, we illustrate the all-possible stable configurations in this section for different planes. For that, we calculate and compare the energies of the all-possible $4\times2 = 8$ configurations based on the Hamiltonian (1). Figure 2 shows the all-stable configurations found in the ground state phase diagrams in the planes (H, D), (H, J_{11}), (H, J_{12}), (D, J_{12}), and (J_{11}, J_{12}) in the absence of any temperature. Figure 2(a) shows the plane (H, D) for fixed values of the physical parameters $J_{11} = J_{22} = J_{12} = 1$. We observe a perfect symmetry in this figure regarding the axis $H = 0$. The variation of the crystal field affects the spins values. While, increasing the external magnetic field affects the sign of the spins. The same behavior is reported in the plan (H, J_{11}) corresponding to Fig. 2(b). When fixing the crystal field $D = 1$, the exchange coupling interactions $J_{11} = J_{22} = 1$ in the plan (H, J_{12}), Fig. 2(c), we find that the exchange coupling interaction J_{12} does not have any impact on the spins S of the Mn atoms. Although, increasing this parameter affects the sign of the spins σ. In the plane (D, J_{12}), see Fig. 2(d), a perfect symmetry is observed between the phases $\pm1/2$ and $\pm3/2$ regarding the axis $J_{12} = 0$. Nevertheless, increasing the crystal field increases the spins S. The same symmetry is shown in Fig. 2(e), plotted in the plan (J_{11}, J_{12}). We note from this figure that the exchange coupling interaction J_{12} affects the sign of the spins while J_{11} influences only the spins S.

In order to inspect the effect of different physical parameters such as the exchange coupling interactions, the temperature, the crystal field, and the external magnetic fields on the total magnetizations of the double perovskite ceramics La_2CuMnO_6, we carried out Monte Carlo simulations under Metropolis algorithm. Based on the Hamiltonian (1), we calculated 10^5 Monte Carlo steps at each spin configuration. We discard the first 10^4 generated configurations. We visited all the sites of the system, and we flipped each spin. The flips are accepted or rejected according to the well-known probability of the Boltzmann statistics.

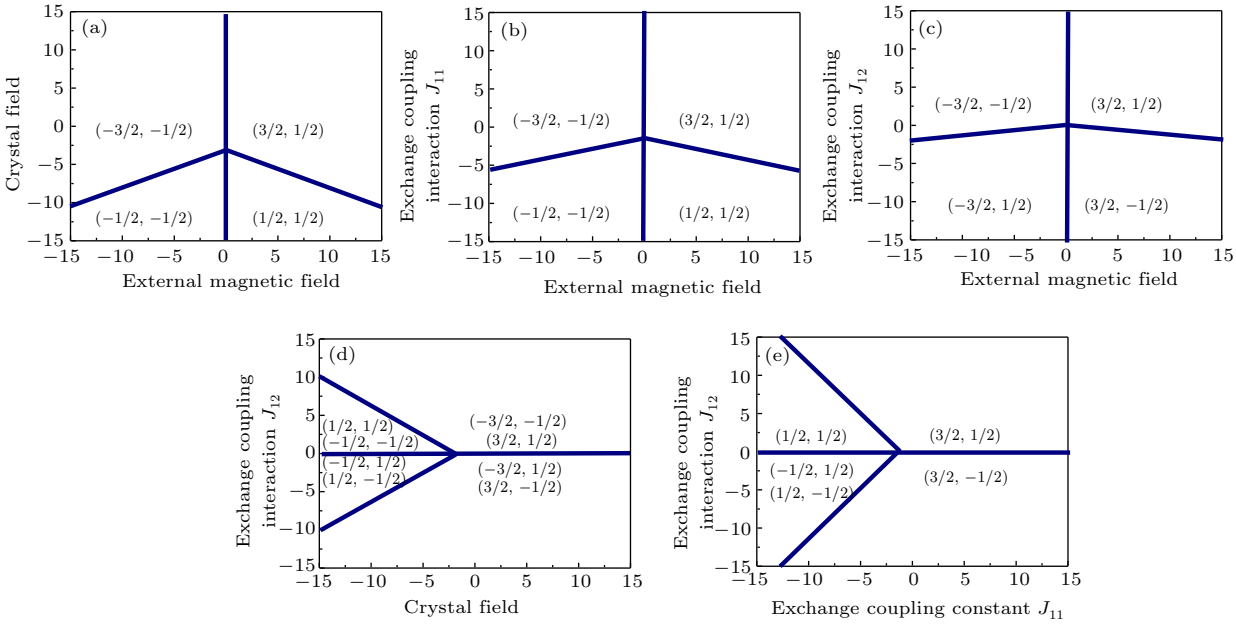


Fig. 2. Ground state phase diagrams of the compound La_2CuMnO_6 in different planes: (a) in the plane (B, D) for $J_{11} = J_{12} = J_{22} = 1$; (b) in the plane ($H$, J_{11}) for $J_{12} = J_{22} = 1$ and $D = 1$; (c) in the plane (B, J_{12}) for $J_{11} = J_{22} = 1$ and $D = 1$; (d) in the plane (D, J_{12}) for $J_{11} = J_{22} = 1$ and $B = 0$; and (e) in the plane (J_{11}, J_{12}) for $J_{22} = 1$, $D = 1$, and $B = 0$.

We illustrate in Fig. 3 the effect of the temperature on the total magnetization and susceptibility, in the absence of the external magnetic fields $H = 9$, for the fixed coupling exchange interactions and the crystal field $J_{11} = J_{12} = J_{22} = 10$ and $D = 10$, respectively. We note a second order transition for the magnetization and susceptibility curves in this figure. The system transits from the ferromagnetic phase to the paramagnetic phase at the critical temperature $T_c = 70$ K, which is in good agreement with the experimental value.[18]

To examine the effect of the competition between the crystal field and the temperature on the total magnetization, we present such behavior in Fig. 4(a), for different selected temperatures: $T = 3$ K, 6 K, and 10 K for $J_{11} = J_{12} = J_{22} = 1$ and $H = 0$. It is found from this figure that the temperature effect is negligible for large negative and positive values of D. On the other hand, for small values of D, the temperature effect is to delay the saturation of the magnetization.

Exploring the effect of varying both the crystal field D and the exchange coupling interaction J_{11}, we show in Fig. 4(b) the obtained results for $T = 3$ K and the exchange coupling values $J_{12} = J_{22} = 1$, and for different values of $J_{11} = -3$, 1, and 3. In the region of negative values of the crystal field, the exchange coupling interaction J_{11} is dominant. While in the positive region of the crystal field, this parameter overrides the coupling interaction exchange except for the negative value of J_{11}. The same behavior is reported when varying J_{12}, see Fig. 4(c). Moreover, the saturation of the magnetization for the antiferromagnetic phase ($J_{12} = -3$) is about $M_T = 0.5$.

We study the effect of the competition between J_{22} and D for the selected values of the exchange coupling interactions $J_{11} = J_{12} = 1$, for $T = 3$ and for different values of $J_{22} = -3$, 1, and 3. The curves shown in Fig. 4(d) demonstrate that the effect of the J_{22} parameter is negligible, since all the curves overlap regardless the value of this parameter.

To inspect the effect of the competition between the temperature and the exchange coupling interaction J_{11}, we report in Fig. 5(a) such behavior for the exchange coupling interaction values of $J_{12} = J_{22} = 1$, the crystal value $D = 3$, and the selected temperature $T = 3$ K, 6 K, and 10 K. From this figure we note that the effect of the temperature is important and is to delay the saturation of the magnetization.

To examine the effect of the crystal field D and the exchange coupling interaction J_{11}, we plot in Fig. 5(b) the obtained results for $J_{12} = J_{22} = 1$ and $D = -3$, 3, 6. It is found that the crystal field has an important impact on the magnetization, for positive values of D the magnetization saturates in positive value ($M_T = 1$). While for negative value of D the saturation of the magnetization takes a negative value ($M_T = -1$).

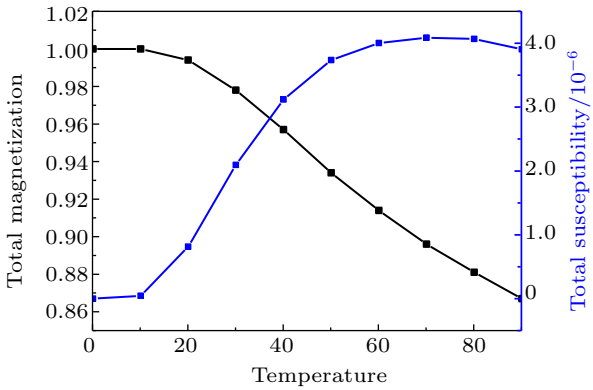


Fig. 3. Total magnetization and total susceptibility as a function of temperature for the fixed coupling interaction values $J_{11} = J_{22} = J_{12} = 10$ and the crystal field value $D = 10$, in the absence of any external magnetic fields $H = 0$.

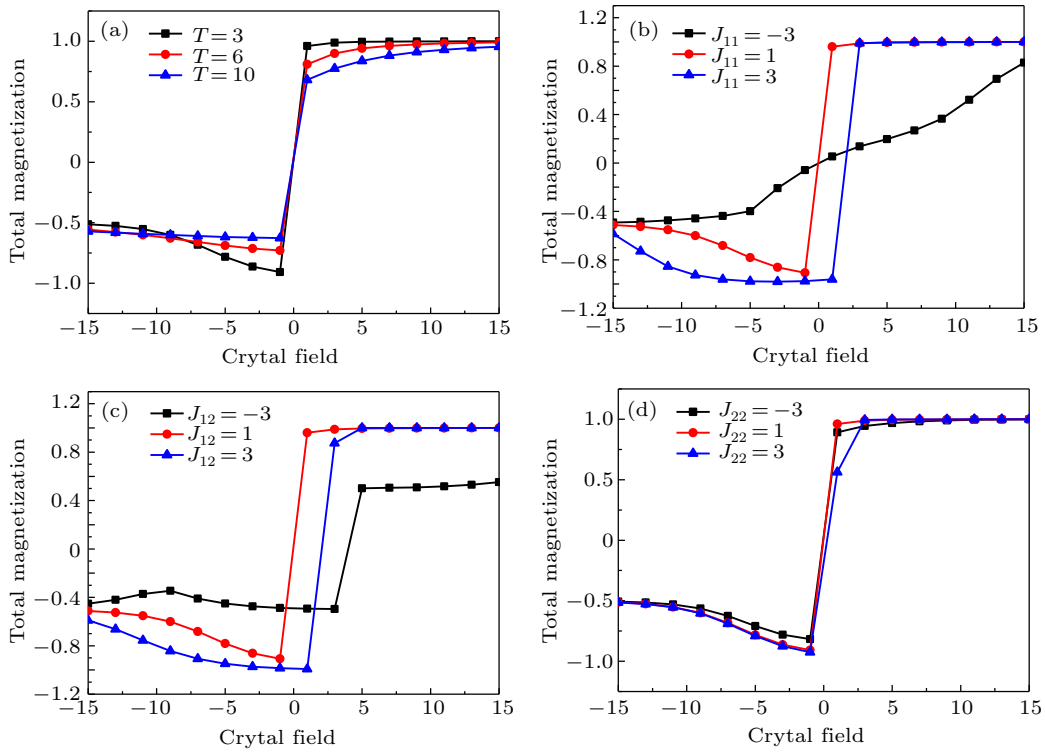


Fig. 4. The total magnetization versus the crystal field in the absence of the external magnetic field $H = 0$, (a) for the selected values of the exchange coupling $J_{11} = J_{12} = J_{22} = 1$ at $T = 3$ K, 6 K, and 10 K; (b) for the exchange coupling values $J_{12} = J_{22} = 1$, the fixed temperature $T = 3$ K, and different values of $J_{11} = -3$, 1, and 3; (c) for the fixed temperature $T = 3$ K, the selected values of the exchange coupling $J_{11} = J_{22} = 1$, and different values of $J_{12} = -3$, 1, and 3; (d) for the selected values of the exchange coupling $J_{11} = J_{12} = 1$, $T = 3$, and different values of $J_{22} = -3$, 1, and 3.

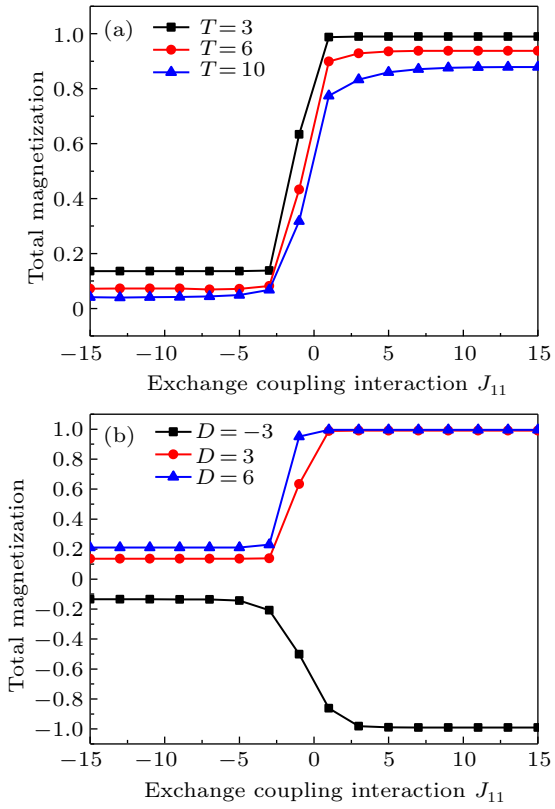


Fig. 5. Total magnetization vs. exchange coupling interaction in the absence of the external magnetic field for (a) $J_{12} = J_{22} = 1$, $D = 3$, and the selected temperature $T = 3$ K, 6 K, and 10 K, (b) $J_{12} = J_{22} = 1$ and different values of $D = -3$, 3, and 6.

The hysteresis loops at 3 K, 5 K, and 7 K are shown in Fig. 6(a). The low-temperature loops are non-saturating at $H = 10$ due to the presence of competing magnetic interactions. An offset regarding the axis $H = 0$ is observed, this is due to the exchange bias.[28] From this figure, the double perovskite ceramics La_2CuMnO_6 is a soft material and can be used for storage devices.

To inspect the behavior of the total magnetization versus the external magnetic field, we plot in Fig. 6(b) the obtained hysteresis loops for $T = 7$ K, $J_{11} = J_{12} = J_{22} = 1$, and $D = -6$, -3, and 3. The reverse behavior to that shown in Fig. 6(a) is observed in this figure keeping the offset regarding the axis $H = 0$. We note for the large negative value of crystal field $D = -6$, the apparition of steps due to the antiferromagnetic behavior.

In Fig. 6(c), $T = 7$ K, $J_{12} = J_{22} = 1$, $D = 3$, and $J_{11} = -5$, -3, and 3. The hysteresis loops show small coercivity indicating the presence of ferromagnetic behavior for $J_{11} = 3$ and antiferromagnetic behavior for $J_{11} = -3$, while it is almost linear showing that the system is completely paramagnetic at $J_{11} = -5$.

To show the effect of varying the exchange coupling interaction between Mn and Cu atoms J_{12}, we illustrate in Fig. 6(d) such behavior for $T = 7$ K, $J_{11} = J_{22} = 1$, $D = 3$, and $J_{12} = -5$, -3, and 1. It is found that both the remanent magnetization and the corresponding coercive magnetic field H_c decrease when increasing the exchange coupling interaction J_{12}.

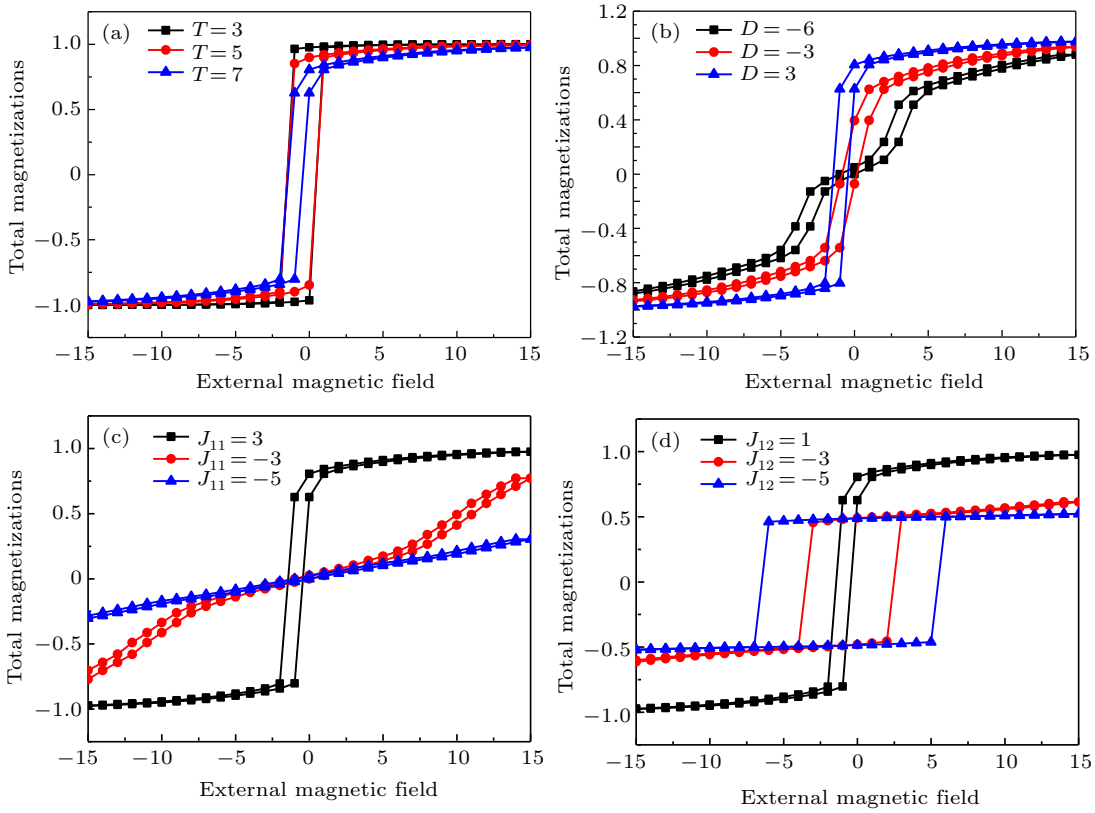


Fig. 6. Total magnetization vs. external magnetic field (a) for $J_{11} = J_{12} = J_{22} = 1$, $D = 3$, and $T = 3$, 5, 7; (b) for $T = 7$ K, $J_{11} = J_{12} = J_{22} = 1$, and $D = -6$, -3, 3; (c) for $T = 7$ K, $J_{12} = J_{22} = 1$, $D = 3$, and $J_{11} = -5$, -3, 3; (d) for $T = 7$ K, $J_{11} = J_{22} = 1$, $D = 3$, and $J_{12} = -5$, -3, 1.

4. Conclusion

In this work, the ground state phase diagrams and the magnetic behavior of the double perovskite ceramics La_2CuMnO_6 have been analyze and discussed exploring Monte Carlo method. The effect of varying the physical parameters such as the exchange coupling interactions J_{12}, J_{22}, J_{11}, the crystal and external fields on the magnetization of the system have been investigated. It is found that the critical temperature of the system is about $T_c = 70$ K. The hysteresis cycle loops have also been studied and showed that, this compound has a soft behavior and can be used in spintronic devices, especially for magnetic recording.

References

[1] Dass R I and Goodenough J B 2003 *Phys. Rev. B* **67** 014401

[2] Rogado N S, Li J, Sleight A W and Subramanian M A 2005 *Adv. Mater.* **17** 2225

[3] Newnham R E and Ruschau G R 1991 *J. Am. Ceram. Soc.* **74** 463

[4] Goldschmidt V M 1926 *Naturwissenschaften* **14** 477

[5] Anderson M T, Greenwood K B, Taylor G A and Poppelmeier K R 1993 *Prog. Solid State Chem.* **22** 197

[6] Howard C J, Kennedy B J and Woodward P M 2003 *Acta Crystallogr. Sect. B: Struct. Sci.* **59** 463

[7] Fiebig M 2005 *J. Phys. D* **38** R123

[8] Eerenstein W, Mathur N D and Scott J F 2006 *Nature* **442** 759

[9] Mtouguia S, Khalladia R, Zitib S, Labrimc H and Bahmad L 2018 *Superl. Micro.* **123** 111

[10] Mtougui S, Khalladi R, El Mekkaoui N, El Housni I, Idrissi S, Bahmad L, Ziti S and Labrim H 2018 *Comput. Cond. Mat.* **17** e00329

[11] Mtougui S, Khalladi R, El Mekkaoui N, El Housni I, Idrissi S, Ziti S, Labrim H and Bahmad L 2018 *Comput. Cond. Mat.* **17** e00331

[12] Mtougui S, El Mekkaoui N, Ziti S, *et al.* 2019 *Appl. Phys. A* **125** 491

[13] Fan X, Wang Y and Jiang Y 2011 *J. Alloys Comp.* **509** 6652

[14] Cortés-Gil R, Ruiz-González M L, Alonso J M, García-Hernández M, Hernando A and González-Calbet J M 2013 *Chem. Mater.* **25** 2100

[15] Patiala and Punjab 2013 *Solid State Physics: Proceedings of the* 58*th DAE Solid State Physics Symposium* 2013 Thapar University, India 17–21 December 2013, AIP Conference Proceedings, Vol. **1591**

[16] Singh D N, Sinha T P and Mahato D K 2017 *Mater. Today: Proc.* **4** 5640

[17] Palakkal J P, Sankar C R, Paulose A P, Valant M, Badasyan A and Varma M R 2018 *Mater. Res. Bull.* **100** 226

[18] Landau D P and Binder K 2009 *A Guide to Monte Carlo Simulations in Statistical Physics* (New York: Cambridge University Press)

[19] El Mekkaoui N, Idrissi S, Mtougui S, *et al.* 2019 *Appl. Phys. A* **125** 582

[20] Idrissi S, Ziti S, Labrim H, Khalladi R, Mtougui S, El Mekkaoui N, El Housni I and Bahmad L 2019 *Phys. A: Stat. Mech. Its Appl.* **527** 121406

[21] Khalladi R, Labrim H, Idrissi S, Mtougui S, El Housni I, Ziti S, El Mekkaoui N and Bahmad L 2019 *Solid State Commun.* **290** 42

[22] El Housni I, Labrim H, El Mekkaoui N, Idrissi S, Khalladi R, Mtougui S, Ziti S and Bahmad L 2019 *SPIN* **9** 1950002

[23] Momma K and Izumi F 2011 *J. Appl. Crystallogr.* **44** 1272

[24] Huo L, Huang W C, Yan Z B, Jia X T, Gao X S, Qin M H and Liu J M 2013 *J. Appl. Phys.* **113** 073908

[25] Huang W C, Huo L, Tian G, Qian H R, Gao X S, Qin M H and Liu J M 2012 *J. Phys.: Condens. Matter* **24** 386003

[26] Qin M H, Zhang G Q, Wang K F, Gao X S and Liu J M 2011 *J. Appl. Phys.* **109** 07E103

[27] Meyl M and Ehresmann A 2020 *J. Magn. Magn. Mater.* **495** 165859

[28] Lee C H, Anbalagan A K, Chang T W, *et al.* 2019 *Mater. Lett.* **254** 309